

The Archaeological Heritage of Oman

THE FIRST PEOPLES OF OMAN

Palaeolithic Archaeology of the Nejd Plateau

JEFFREY I. ROSE, YAMANDÚ H. HILBERT
ANTHONY E. MARKS & VITALY I. USIK



Sultanate of Oman
Ministry of Heritage and Culture



ARCHAEOPRESS PUBLISHING LTD
Summertown Pavilion
18-24 Middle Way
Summertown
Oxford OX2 7LG
www.archaeopress.com

© Jeffrey I. Rose, Yamandú H. Hilbert, Anthony E. Marks & Vitaly I. Usik 2019

The First Peoples of Oman. Palaeolithic Archaeology of the Nejd Plateau
(Includes bibliographical references and index).

1. Arabia. 2. Oman. 3. Dhofar. 4. Nejd Plateau. 5. Palaeolithic. 6. Stone tools.

This edition is published by Archaeopress Publishing Ltd in association with the Ministry of
Heritage and Culture, Sultanate of Oman.

Printed in England

ISBN 978-1-78969-284-6
ISBN 978-1-78969-285-3 (e-Pdf)

This publication is in copyright. Subject to statutory exception and to the provisions of relevant
collective agreements, no reproduction of any part may take place without the written permission of
the Ministry of Heritage and Culture, Sultanate of Oman.

Ministry of Heritage and Culture
Sultanate of Oman, Muscat
P.O. Box 668 P.C. 100
Khuwair, Muscat
Phone: +968 24 64 13 00
Fax: +968 24 64 13 31
Email: info@mhc.gov.om
Web Site: www.mhc.gov.om

Cover image: A stone workshop site in Wadi Haluf, central Dhofar (photograph by the Dhofar
Archeological Project).

Contents

<i>List of illustrations and tables</i>	v
<i>Acknowledgments</i>	xiii
<i>Preface</i>	xv
1 Geography and palaeoenvironments	1
2 The Lower Palaeolithic in Dhofar	16
3 The Middle Palaeolithic in Dhofar	53
4 The Upper and Late Palaeolithic in Dhofar	107
5 Conclusions and avenues for future research	168
<i>Bibliography</i>	180
<i>Index</i>	193

List of illustrations

FIGURES

1.1.	Map of southern Arabia showing regions mentioned in the text.	2
1.2.	The Al-Hajar Mountains near Wadi Al-Ain (photograph by the authors).	3
1.3.	Panorama of farming terraces on Jebel Akhdar (photograph by the authors).	4
1.4.	Archaeological survey near Adam in central Oman (photograph by the authors).	6
1.5.	Salalah coastal plain with the Dhofar Mountains on the right (photograph by the authors).	7
1.6.	Landscape east of Mirbat showing rhyolite dykes (photograph by the authors).	8
1.7.	Wadi Darbat during the monsoon season (photograph by the authors).	10
1.8.	Vegetation on the flanks of the Dhofar Mountains (photograph by the authors).	11
1.9.	View from the Dhofar orographic barrier facing north towards the Nejd Plateau (photograph by the authors).	11
1.10.	Scablands on the southern Nejd Plateau in the vicinity of Wadi Haluf (photograph by the authors).	12
1.11.	Raw material outcrops found across Dhofar (above); dense carpet of chert artifacts above Wadi Ghadun close to Mutahafah (below); chert nodules outcropping from the limestone bedrock of the Nejd (photographs by the authors).	13
1.12.	Panorama over Wadi Aybut on the west-central Nejd (photograph by the authors).	14
1.13.	The northern Nejd Plateau near Shisr Farms (photograph by J.M. Geiling).	14
1.14.	Sand dunes north of Al-Hashman in the southern Rub Al-Khali (photograph by the authors).	15
2.1.	Map of the Arabian Peninsula showing key Lower Palaeolithic sites.	19
2.2.	Handaxes from (1) Al-Garb VII and (2, 3) Djob-Hamid 1 (after Amirkhanov 1987: fig. 8).	21
2.3.	Weathering patterns on a Lower Palaeolithic biface versus a Middle Holocene biface from the same locality (photographs by the authors).	23
2.4.	Isolated handaxe finds (photographs by the authors).	23
2.5.	Map showing the position of Lower Palaeolithic isolated handaxes and foliate findspots recorded by the DAP.	24
2.6.	Map showing the location of all Lower Palaeolithic findspots recorded by the DAP: isolated handaxes, isolated foliates, late Lower Palaeolithic blade sites and Acheulean sites.	25
2.7.	Map showing the location of Lower Palaeolithic sites (gray squares) and isolated handaxes (red triangles) on the central-western Nejd Plateau.	27
2.8.	Volumetric cores from TH.501a: (1) core showing blade scar reduced in semi-tournant manner and (2) core showing flake negatives produced on nodule reduced in unidirectional-parallel manner (photographs by Y.H. Hilbert).	28

2.9.	Flat cores from TH.501a: (1-4) discoid cores, (2) flat unidirectional-lateral core, (3) flat core with bilateral distal negatives on the dorsal surface (photographs by Y.H. Hilbert).	29
2.10.	Impact marks on the distal end of a discoid core (#4 in figure 2.9). Such impact marks are typical and indicate that the piece was also used as a percussor (photograph by Y.H. Hilbert).	31
2.11.	Choppers made on chert nodules from TH.501a (photographs by Y.H. Hilbert).	31
2.12.	Handaxes from TH.501a: (1) triangular handaxe with cortical butt and asymmetric edges, (2) lanceolate-shaped handaxe with cortical butt, (3-5) cordiform handaxes (illustrations by Y.H. Hilbert).	32
2.13.	Ovate handaxes from TH.501a: (1) handaxe made on flake, (2-3) handaxe made on nodules (photographs by Y.H. Hilbert).	33
2.14.	Handaxe from TH.501a subsequently used as a unidirectional core. The patination of the artifacts is homogenous, suggesting that the two different uses of the piece were roughly contemporary (photographs by Y.H. Hilbert).	34
2.15.	TH.501a handaxe metrics (figure plots by Y.H. Hilbert).	36
2.16.	Heat map showing the distribution of differentially weathered Lower Palaeolithic artifacts from TH.76 (figure plots by Y.H. Hilbert).	37
2.17.	Handaxes made on cortical blanks from TH.76 (illustrations by Y.H. Hilbert).	38
2.18.	Cores from TH.76: (1) unidirectional single platform core reduced in semi-tournant manner, (2) unidirectional parallel single platform flat core, (3) discoid core (photographs by Y.H. Hilbert).	39
2.19.	Handaxes from TH.76: (1) thick sub-triangular, (2) amygdaloid on flat nodule, (3) small asymmetrical ovate, (4) large lanceolate with cortical butt, (5,6) symmetrical ovate handaxes (photographs by Y.H. Hilbert).	40
2.20.	Handaxes from TH.76: (1) handaxe subsequently used as core, the butt was removed by unidirectional-parallel removals, (2) symmetrical amygdaloid handaxe with tip removed by a series of removals oriented transverse to the technological axis of the artifact, (3) handaxe with tip removed by blows to the edge (photographs by Y.H. Hilbert).	41
2.21.	Panorama overlooking the Jebel Sanoora terraces (photograph by the authors).	42
2.22.	Unidirectional-parallel cores from TH.143 (photographs by Y.H. Hilbert).	44
2.23.	Unidirectional-parallel blades from TH.143 (photographs by Y.H. Hilbert).	44
2.24.	TH.143 blade and core metrics (figure plot by Y.H. Hilbert).	45
2.25.	Panorama overlooking Wadi Khasheem with TA.23 site located inside the red dotted line (photograph by the authors).	46
2.26.	Surface of the Wadi Khasheem terrace (photograph by the authors).	47
2.27.	Lower Palaeolithic artifacts from TA.23: (1-4) flakes, (2) single platform core, (3) retouched cortical flake, (5) massive discoid core (photographs by Y.H. Hilbert).	49
2.28.	Débitage from TA.23 (illustrations by A. Beshkani).	50
2.29.	Tools and cores from TA.23 (illustrations by A. Beshkani).	51
3.1.	Preferential Levallois flake cores from northern Saudi Arabia after Hilbert <i>et al.</i> (2015a).	54
3.2.	Schema of preferential centripetal Levallois, unidirectional convergent Levallois and Nubian Levallois methods after Crassard and Hilbert (2013).	56

3.3.	Map showing the location of Nubian Complex occurrences across North Africa and the Arabian Peninsula after Hilbert <i>et al.</i> (2016).	58
3.4.	Map showing the location of Middle Palaeolithic findspots recorded by the Dhofar Archaeological Project between 2010 and 2013.	59
3.5.	TH.418 upper terrace (photograph by the authors).	60
3.6.	Topographic map of TH.418 (figure plot by Y.H. Hilbert).	61
3.7.	Spatial distribution plot of Middle Palaeolithic and Late Palaeolithic artifacts collected at TH.418 (figure plot by Y.H. Hilbert).	62
3.8.	Nubian Middle Palaeolithic artifacts from TH.418: (1-3) Nubian Levallois points, (4) débordant blade, (5-12) Nubian Levallois cores (photographs by A. Beshkani).	64
3.9.	Nubian Middle Palaeolithic artifacts from TH.418: (1-4) Nubian Levallois cores, (2) Levallois flake with discontinuous lateral retouch, (3) Nubian Levallois point, (5) notch (illustrations by Y.H. Hilbert).	65
3.10.	Bidirectional Middle Palaeolithic cores from TH.418 (photographs by A. Beshkani).	66
3.11.	Bidirectional Middle Palaeolithic cores from TH.418: (1) bidirectional Levallois core on narrow surface of plaquettes, (2) bidirectional Levallois core, (3) exhausted bidirectional blade core (illustrations by Y.H. Hilbert).	67
3.12.	Spatial distribution plot of Middle and Late Palaeolithic artifacts from TH.419 (figure plot by Y.H. Hilbert).	68
3.13.	Nubian Levallois cores and products from TH.419: (1-3) Nubian Levallois points, (4-9) Nubian Levallois cores (photographs by A. Beshkani).	71
3.14.	Bidirectional cores from TH.419: (1-2) bidirectional blade cores, (3) bidirectional Levallois core, (4) bidirectional Levallois core made on darker patinated flake (photographs by A. Beshkani).	72
3.15.	Bidirectional Levallois cores from TH.419 (photographs by A. Beshkani).	73
3.16.	Late Palaeolithic blade scatter at TH.123 (photograph by the authors).	74
3.17.	TH.123 surface collection area prior to sampling in 2011 (photograph by the authors).	75
3.18.	TH.123 surface collection during sampling in 2011 (photograph by the authors).	75
3.19.	More heavily weathered Nubian cores from TH.123 (photographs by A. Beshkani).	76
3.20.	Less heavily weathered Nubian artifacts from TH.123: (1) Levallois blade, (2) Levallois point, (5) Levallois flake fragment with rootlet patina on the ventral side, (3,6) Nubian Levallois cores, (4) Levallois core (photographs by A. Beshkani).	77
3.21.	Spatial distribution plot of Middle and Late Palaeolithic artifacts from TH.123 (figure plot by Y.H. Hilbert).	78
3.22.	Topographic map of TH.143 showing locations of systematic collection areas and location of transect where the artifacts were piece-plotted (figure plot by Y.H. Hilbert).	80
3.23.	Spatial distribution plot of Middle Palaeolithic and Late Palaeolithic artifacts from TH.143 (figure plot by Y.H. Hilbert).	81
3.24.	Nubian Levallois cores from TH.143 (photographs by A. Beshkani).	82
3.25.	Nubian Levallois cores from TH.143 (photographs by A. Beshkani).	83
3.26.	Middle Palaeolithic tools from TH.143: (1) denticulate, (2-4) sidescrapers (photographs by A. Beshkani).	84

3.27.	Spatial distribution plot of Middle Palaeolithic artifacts from TH.76 showing refittings (figure plot by Y.H. Hilbert).	85
3.28.	Nubian Levallois points from TH.76 (photographs by A. Beshkani).	87
3.29.	More heavily weathered Nubian cores from TH.76 (photographs by A. Beshkani).	88
3.30.	Less heavily weathered Middle Palaeolithic artifacts from TH.76: (1-3) bidirectional Levallois cores, (2) Nubian Levallois core; 4) Recurrent bidirectional blade core (photographs by A. Beshkani).	89
3.31.	Refittings from TH.76: (A) fragmented Nubian Levallois core and point, (B) Nubian Levallois core and point, (C) distal preparation removal conjoined to Nubian Levallois core (photographs by A. Beshkani).	90
3.32.	Refittings from TH.76. Nubian core and point with distal preparation débordant blade (photographs by A. Beshkani).	91
3.33.	Topographic map of Jebel Najm showing the location of the TH.268 systematic collection area (figure plot by Y.H. Hilbert).	92
3.34.	Jebel Najm. View of the site showing the location of the TH.268 collection area in the back adjacent to the dense chert outcrop (photograph by the authors).	94
3.35.	Jebel Najm. View of the site showing the location of the TH.268 collection area (photograph by the authors).	95
3.36.	Middle Palaeolithic cores from TH.268: (1-3) Nubian Levallois cores, (4,6) bidirectional Levallois cores, (5) Nubian Levallois core during re-preparation, (7,8) single platform unidirectional blade cores on narrow surface of nodule, (9,10) bidirectional recurrent blade cores (photographs by Y.H. Hilbert).	96
3.37.	Small Nubian Type 2 Levallois cores from TH.268 (illustrations by Y.H. Hilbert).	97
3.38.	Small Nubian Type 1 Levallois cores from TH.268 (illustrations by Y.H. Hilbert).	98
3.39.	Other Levallois and non-Levallois cores from TH.268: (1,2,7) Levallois cores, (3) single platform unidirectional-parallel core on narrow surface, (4) single platform unidirectional core, (5) bidirectional recurrent blade core with faceted platforms, (6) flat single platform unidirectional flake core (illustrations by Y.H. Hilbert).	99
3.40.	Views of TH.191: top of the inselberg (photograph by the authors).	100
3.41.	Views of TH.191: inselberg seen from a distance (photograph by the authors).	101
3.42.	Views of TH.191: edge of site rising over the plain (photograph by the authors).	101
3.43.	Artifacts and refittings from TH.191. A1 and B1 refittings: (1) single platform unidirectional core on narrow surface with crest preparation, (2) Levallois core with distal overpassed termination from which an additional rectangular preferential flake has been removed (illustrations by Y.H. Hilbert).	103
3.44.	Nubian Levallois cores from TH.191 (illustrations by Y.H. Hilbert).	104
3.45.	Artifacts and refittings from TH.191. A1 and B1 refittings: (1) single platform unidirectional core on narrow surface with crest preparation, (2) Levallois core with distal overpassed termination from which an additional rectangular preferential flake has been removed (illustrations by Y.H. Hilbert).	105
4.1.	Map showing the location of dated Upper and Late Palaeolithic sites in southern Arabia.	108
4.2.	Map showing the location of Upper and Late Palaeolithic findspots recorded by the Dhofar Archaeological Project between 2002 and 2013.	109

4.3.	Burins from Late Palaeolithic sites on the southern Nejd Plateau (after Hilbert <i>et al.</i> 2018).	112
4.4.	Use-wear traces on burins from TH.413 (after Hilbert <i>et al.</i> 2018).	113
4.5.	View of Jebel Kareem (photograph by the authors).	114
4.6.	Terraces at the foot of Jebel Kareem (photograph by the authors).	114
4.7.	Surface of the top of Jebel Kareem (photograph by the authors).	116
4.8.	The DAP team making systematic collections from TH.68 (photograph by the authors).	116
4.9.	View from the top of the inselberg (photograph by the authors).	117
4.10.	Topographic map of TH.68 showing the higher density area (red), lower density area (yellow) and collection areas (blue) (figure plot by Y.H. Hilbert).	119
4.11.	Middle Palaeolithic artifacts from TH.68: (1-3) Levallois blanks into tools retouched during a subsequent phase of usage, (4,5) Middle Palaeolithic cores (photographs by Y.H. Hilbert).	120
4.12.	Upper Palaeolithic tools from TH.68: (1) Composite end scraper and burin on truncation, (2-4) backed bladelets, (5) plano-convex bifacial point, (6) unifacial point, (7) partly-unifacial point, (8) preform, (9) shouldered end scraper (photographs by Y.H. Hilbert).	121
4.13.	Carinated core from TH.68 (photograph by Y.H. Hilbert).	122
4.14.	Blade debitage from TH.68 (illustrations by Y.H. Hilbert).	124
4.15.	Bladelet cores from TH.68 (illustrations by Y.H. Hilbert).	125
4.16.	Upper Palaeolithic cores from TH.68: (1) refit core on flake (2) core on flake, (3) unidirectional single platform bladelet core, (4,5) unidirectional single platform blade cores (illustrations by Y.H. Hilbert).	126
4.17.	TH.68 segment refittings (photographs by Y.H. Hilbert).	127
4.18.	TH.68 burins made on snapped segments (illustrations by Y.H. Hilbert).	128
4.19.	Multiple and single burins on truncation from TH.68 (illustrations by Y.H. Hilbert).	130
4.20.	Bifacial and unifacial tools from TH.68 (illustrations by Y.H. Hilbert).	131
4.21.	Upper Palaeolithic tools from TH.68: (1-7) backed bladelets, (8) unifacial point, (9,13,14,16,18) end scrapers, (10) awl, (11) laterally retouched blade, (12) denticulate, (15) piercer, (17) retouched bladelet (illustrations by Y.H. Hilbert).	132
4.22.	DAP team systematically collecting findspot TH.262 (photograph by J.M. Geiling).	133
4.23.	TH.262 blade cores (illustrations by Y.H. Hilbert).	134
4.24.	TH.262 core-on-flake refittings (illustrations by Y.H. Hilbert).	135
4.25.	TH.262 tools: (1) piercer, (2,3) ogival end scrapers, (4) bifacial foliate, (5) bifacial preform, (6) retouched blade (illustrations by Y.H. Hilbert).	137
4.26.	TH.143 Late Palaeolithic collection area (photograph by the authors).	138
4.27.	TH.143 artifacts: (1-8) Late Palaeolithic blade debitage, (9) retouched blade (illustrations by Y.H. Hilbert).	141
4.28.	TH.143 Late Palaeolithic biface and bifacial thinning elements (illustrations by Y.H. Hilbert).	143
4.29.	TH.38 Late Palaeolithic collection area near Shisr Farms (photograph by the authors).	144

4.30.	Artifacts from TH.38 (photographs by Y.H. Hilbert).	147
4.31.	Debitage from TH.38 (illustrations by Y.H. Hilbert).	150
4.32.	Debitage from TH.38 (illustrations by Y.H. Hilbert)	151
4.33.	Cores from TH.38: (1,3,4) single platform unidirectional cores, (2) perpendicular core (illustrations by Y.H. Hilbert).	153
4.34.	Large flake cores from TH.38 (illustrations by Y.H. Hilbert).	154
4.35.	Large bidirectional opposed platform cores from TH.38 (illustrations by Y.H. Hilbert).	154
4.36.	Debitage from TH.38 with complex scar patterns (illustrations by Y.H. Hilbert).	155
4.37.	TH.38: Blade core refitting A (illustrations by Y.H. Hilbert).	156
4.38.	TH.38: Blade core refittings B (illustrations by Y.H. Hilbert).	157
4.39.	TH.38: Blade core refittings C (illustrations by Y.H. Hilbert).	157
4.40.	Tools from TH.38: (1) bifacial preform, (2,3) retouched blanks, (4) side scraper, (5) bifacial fragment (illustrations by Y.H. Hilbert).	158
4.41.	View towards the south from the Al-Hatab Rockshelter (photograph by the authors).	159
4.42.	Surface plot of Al-Hatab showing the location of TH.29 excavation areas and TH.34 surface collection area (figure plot by Y.H. Hilbert).	159
4.43.	Debitage from TH.34 (illustrations by Y.H. Hilbert).	162
4.44.	Blade cores from TH.34 (illustrations by Y.H. Hilbert).	163
4.45.	Multiple platform cores from TH.34 (illustrations by Y.H. Hilbert).	164
4.46.	TH.34 refittings: (A1, A2) blade core with débordant refits, (B1, B2) blade core with thick lateral refit (illustrations by Y.H. Hilbert)	165
4.47.	Tools from TH.34: (1-3,6) end scrapers, (4,5) retouched blanks, (7-9) burins on truncation, (10,11) dihedral burins, (12) burin on snap (illustrations by Y.H. Hilbert).	167
5.1.	Acheulean artifacts from Dhofar: (1-6) handaxes from the Nejd Plateau and coastal plain, (7,8) Lower Palaeolithic cores (illustrations by A. Beshkani & Y.H. Hilbert).	169
5.2.	Earlier Middle Palaeolithic artifacts from Dhofar: (1-3) Nubian Levallois points, (4-10) Nubian Levallois cores (photographs by Y.H. Hilbert).	171
5.3.	Later Middle Palaeolithic artifacts from Dhofar: (1) bidirectional narrow surface core, (2) unidirectional narrow surface core, (3) unidirectional narrow surface core with ridge preparation, (4,5) bidirectional opposed blade cores, (6-8) Nubian Levallois cores, (9) Levallois preferential cores (illustrations by Y.H. Hilbert).	172
5.4.	Upper Palaeolithic artifacts from TH.68: (1-4) bladelets, (5-7) backed bladelets, (8) burin on truncation, (9,10) shouldered end scrapers, (11) burin on segment, (12) bifacial plano-convex point, (13) end scraper with lateral retouch, (14) unifacial point (15,16) bladelet cores (illustrations by Y.H. Hilbert).	174
5.5.	Late Palaeolithic artifacts from Dhofar: (1-3) blades and débordant blades, (4-6,8,11) end scrapers, (7) ovate biface, (9) dihedral burin, (10) burin on natural surface, (12) Wa'shah core, (13) unidirectional-parallel semi-tournant blade core (illustrations by Y.H. Hilbert).	175
5.6.	Palaeolithic artifacts showing different stages of weathering: (1,2) Lower Palaeolithic, (3-5) earlier Middle Palaeolithic, (6-8) later Middle Palaeolithic, (9-11) Late Palaeolithic (photographs by Y.H. Hilbert).	177

- 5.7. Schematic representation of multi-occupation site formation processes showing hypothetical retreat of the scarp due to erosion: (a) Stage 1 shows a typical block section from the Nejd with chert nodules and slabs eroding within, (b) Stage 2 shows the advance of scarp erosion that exposes fresh chert nodules, which were used to produce Lower Palaeolithic stone tools by the initial hominid inhabitants of the Nejd Plateau, (c) Stage 3 shows continued erosion and retreat of the low scarp, which exposes new chert nodules, continuing throughout the Palaeolithic and Holocene. During subsequent stages, successive groups of toolmakers returned to exploit fresh chert nodules eroding from the edge of the scarp (illustration by Y.H. Hilbert). 178

TABLES

3.1.	Artifact counts from TH.418.	63
3.2.	Artifact counts from TH.419.	70
3.3.	Artifact counts from TH.123.	79
3.4.	Artifact counts from TH.143 Middle Palaeolithic component.	80
3.5.	Artifact counts from TH.76 Middle Palaeolithic component.	86
3.6.	Artifact counts from TH.268.	93
3.7.	Core counts from TH.191.	102
4.1.	Artifacts counts from TH.68.	118
4.2.	Débitage scar patterns from TH.68.	118
4.3.	Débitage shapes from TH.68.	118
4.4.	Débitage midpoint cross sections, distal terminations and longitudinal profiles from TH.68.	120
4.5.	Débitage striking platforms from TH.68.	122
4.6.	Débitage metric data from TH.68.	123
4.7.	Core classifications from TH.68.	123
4.8.	Tool classifications from TH.68.	129
4.9.	Artifact counts from TH.262.	136
4.10.	Débitage attributes from TH.262.	138
4.11.	Débitage metric data from TH.262.	139
4.12.	Artifact counts from TH.143 Late Palaeolithic component.	140
4.13.	Débitage attributes from TH.143 Late Palaeolithic component.	142
4.14.	Débitage metric data from TH.143 Late Palaeolithic component.	146
4.15.	Artifact counts from TH.38.	148
4.16.	Débitage attributes from TH.38.	149
4.17.	Débitage metric data from TH.38.	152
4.18.	Artifacts counts from TH.34.	160
4.19.	Débitage attributes from TH.34.	161
4.20.	Débitage metric data from TH.34.	166

Acknowledgements

This volume is the product of over fifteen years of research in the Sultanate of Oman, to which we owe our gratitude to several individuals. First and foremost, we thank His Majesty Sultan Qaboos bin Said Al-Said for cultivating and inspiring the scientific curiosity of a nation. We thank His Royal Highness Sayyid Haitham bin Tarik Al-Said, Minister of Heritage and Culture. We are grateful to the Undersecretary for Heritage, H.E. Salim bin Mohammed Al-Mahrooqi, and the Adviser for Heritage sites, H.E. Hassan bin Mohammed Al-Lawati, as well as to Sultan bin Saif Al-Bakri, Director General for Archaeology. We thank Khamis Al-Asmi in his role as both Director of the Department of Excavations and Archaeological Studies and as a team member during our first Dhofar fieldwork campaign in 2004.

We wish to thank each and every colleague who has dedicated their time and energies to the Dhofar Archaeological Project over the years: Jeanne Marie Geiling, Christopher Galletti, Mohammed Jaboob, Said Al-Saqri, Ali Al-Mahrooqi, Yaqoub Al-Busaidi, Amir Beshkani, Adrian Parker, Michael Morley, Ash Parton, Natalia Pankova, Philip Van Peer, Marta Lahr, Robert Foley, Richard 'Bert' Roberts, Kira Westaway, Laine Clark-Balzan, Matthias Blessing, Ignacio Clemente-Conte, Musallam Al-Mahri, Daniel Richter, Diego Angelucci, Teresa Medici, Kathryn Price and Henry de Santis. This volume is the culmination of all their efforts.

The project was funded by a UK Arts and Humanities Research Council Early Career Research grant (AH/G012733/1) and National Geographic Society Waitt grant (W253-12) awarded to J.I. Rose, as well as a Fondation Fyssen grant awarded to Y.H. Hilbert supporting his post-doctoral research and laboratory analyses. We are particularly grateful to the editor of this series, Dennys Frenez, for his steadfast patience and support throughout the occasionally painful process of writing this book.

In its inception nearly two decades ago, the Dhofar Archaeological Project was made possible by the help and encouragement of Juris Zarins, Joy McCorriston, Dan Potts, Mauro Cremaschi, and H.E. Ali Al-Shanfari, as well as those no longer with us: Maurizio Tosi, Serge Cleuziou, Said Al-Mahri and Norman Whalen. It is with our deepest gratitude and in their memory that we dedicate this work.

Preface

The study of prehistory focuses on the archaeological periods that precede the written word. It is not confined to the past of our own species, but seeks to understand cultural expressions of our ancestors and predecessors. According to the late Hans Jürgen Eggert (1986: 14), “*Prehistory is the science of the shovel*”.

This statement may be fitting for the prehistoric archaeology of Europe, where digging into the ground is how information is typically acquired. This is not the case, however, for the arid landscapes of southern Oman. Over the course of five field seasons, the Dhofar Archaeological Project team walked hundreds and drove thousands of kilometers, collecting well over a metric ton of stone tools scattered on the surface. It is a land of total archaeological visibility, with few preserved sediments. Throughout our entire campaign we used just three shovels, but sacrificed countless shoes and punctures to the flint teeth of the rocky desert. In Oman, it would be more accurate to say prehistory is the science of rubber soles and flat tires.

The First Peoples of Oman – Palaeolithic archaeology of the Nejd Plateau presents the results of our archaeological research in the Governorate of Dhofar between 2010 and 2013. Initially, the aim of the project was to test the rapid coastal migration hypothesis of early modern human expansion out of Africa. Dhofar is an ideal candidate to study this specific route of dispersal, due to its seasonal rainfall, plethora of chert outcrops and karstic cavities riddling the mountain escarpment. The continental shelf in Dhofar remained relatively stable throughout the past, whereas in many other places along the Indian Ocean rim, rising sea levels have submerged ancient coastal landscapes that served as hypothetical corridors of early human migration.

During the first few months of the 2010 campaign, our survey focused on the Dhofar mountain seaward slopes and coastal plain. These were the least productive and most discouraging months of the entire project. We did not find a single Middle, Upper, or Late Palaeolithic site. We tirelessly tested rockshelters, caves and terraces for sediments bearing Palaeolithic cultural remains, without producing a single artifact. On the advice of Juris Zarins, with years of archaeological survey experience in Dhofar, we eventually set our sights on the western Nejd Plateau.

It was there, around the village of Mudayy, at last we struck gold (chert, to be precise). On an ancient terrace above Wadi Aybut, we discovered a stone tool industry made by one of the earliest modern human populations on earth. This was a breakthrough in both our understanding of early human dispersal, as well being able to read the Palaeolithic landscapes of Dhofar. In subsequent campaigns, our team mapped hundreds of prehistoric sites across the region, some multi-occupation sites with evidence of successive habitation for over a million years.

This volume summarizes these findings in five chapters. We begin with an overview of geography and palaeoenvironments, describing the diverse landscapes and fluctuating palaeoenvironmental record of Dhofar. The next three chapters present our discoveries from the Lower, Middle and Upper-Late Palaeolithic archaeological periods. Each chapter begins with a short overview of the major cultural and biological milestones from a global and regional perspective, before describing a sample of findings from the Dhofar Archaeological Project. The final chapter synthesizes these data and considers prospects for future Palaeolithic research in southern Oman.

Chapter 1

Geography and palaeoenvironments

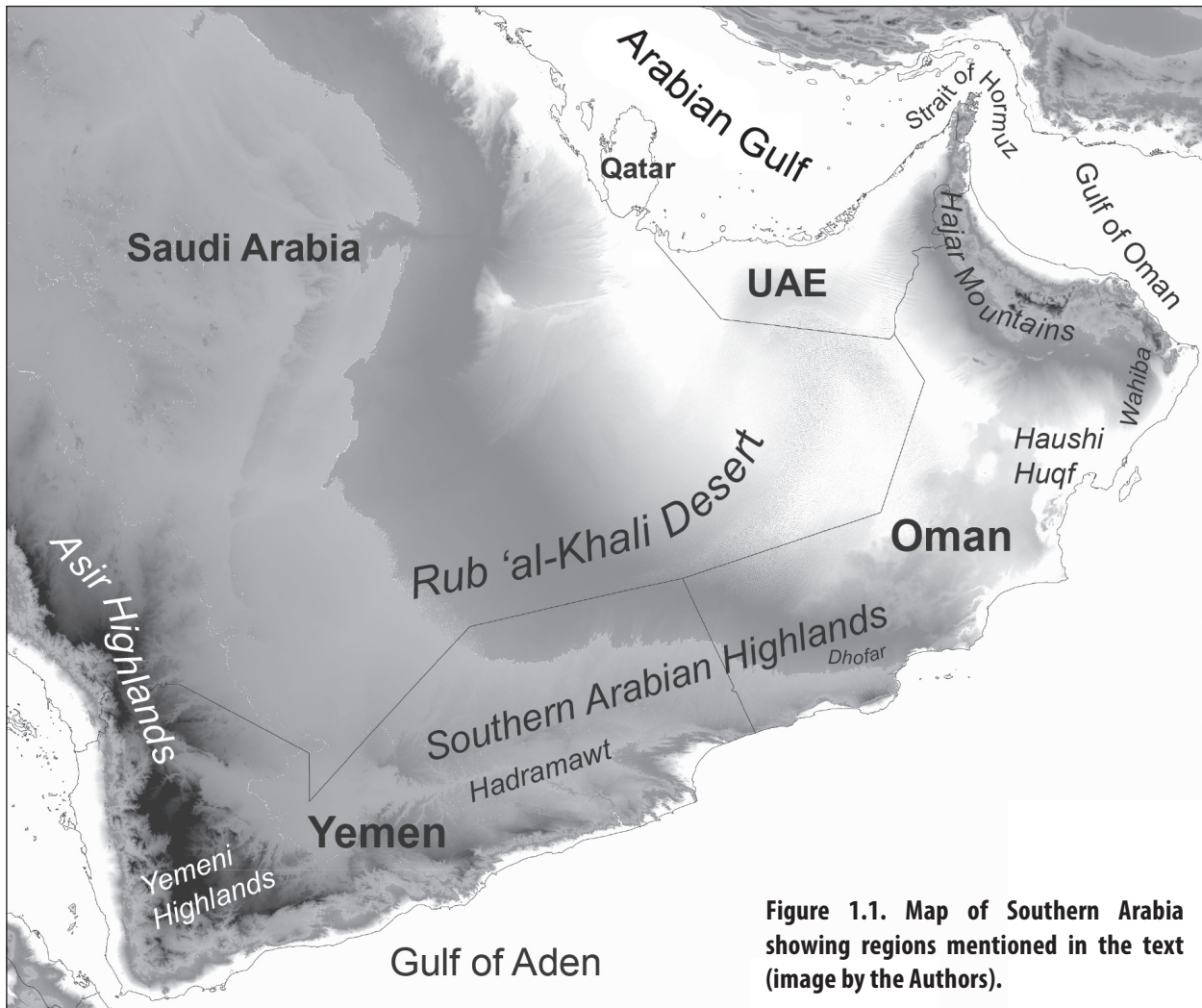
The earth's climate and environments are in a perpetual state of flux. Our planet orbits the sun along an eccentric elliptical path, which alters the amounts of average annual solar radiation we receive over 100,000-year cycles. In addition, the earth wobbles and tilts as it spins on its axis, influencing climatic fluctuations over 41,000 and 26,000-year periods (Milanković 1920). Evidence of these fluctuations are embedded within the landscape, called environmental proxy signals, which are among the most important sources of information for researchers studying early human prehistory and ecology. In and around Oman, such environmental proxy signals include ancient lake sediments in the desert, dust deposits on the sea floor, stalactites dripping from cave ceilings, even the dunes themselves.

With the development of innovative dating techniques in the last few decades that reach beyond the 40,000 year limit of traditional radiocarbon dating, scientists are able to measure the age of calcium carbonate rock, volcanic ash, or the time elapsed since a grain of sand has been exposed to light. Harnessing these various methods for measuring the age of stratified deposits, it is possible to reconstruct the chronology and impact of climate change on the prehistoric landscapes of Oman.

One particularly effective environmental proxy signal comes from deep-sea cores, which store an archive of climate change reaching back several million years. By observing variations over time in the chemical composition of plankton deposited in the seabed, scientists have recorded cyclical fluctuations in the ratio between different oxygen isotopes. These cycles, in turn, are a function of how much of the earth's water is trapped in glaciers. During glacial periods, rainfall rich in ^{16}O was frozen in continental ice sheets that extended down into North America and Europe, skewing the marine isotope ratios toward higher amounts of ^{18}O versus ^{16}O . Conversely, warm periods caused widespread glacial melting that released ^{16}O -rich water into the oceans, all of which are recorded within the calcareous shells of planktonic foraminifera. These cold and warm intervals are referred to as Marine Isotope Stages (MIS), beginning with the most recent MIS 1 and counting backward in time. Odd-numbered isotope stages indicate interglacial periods, when warm and humid conditions prevailed, while even-numbered isotope stages denote glacial periods, when cold and dry climatic conditions enveloped the globe.

Isotope stages can be further divided into sub-stages, such as MIS 5.1, 5.2, 5.3, etc. Sub-stages are either brief periods of a warmer climatic regime during glacial periods (i.e., interstadials) or an episode of global cooling during an interglacial (i.e., stadials) (Anderson *et al.* 2007; Lisiecki and Raymo 2005; Waelbroeck *et al.* 2002).

These glacial-interglacial cycles, known as the ice ages, began 2.58 million years ago at the start of the Quaternary geological period and Pleistocene geological epoch (Gibbard *et al.* 2010). More than 100 marine isotope stages have been identified within the Pleistocene, which lasted for over 2.5 million years. The Pleistocene was characterized by climatic instability and oscillations between warm and cold global temperatures. Fluctuations between warm interglacial and cold glacial periods became increasingly extreme in the latter half of the Pleistocene. The period between 132,000 and 112,000 years ago is referred to as the Last Interglacial (MIS 5.5), dominated by an unusually warm and wet climate across most of the earth (Otvos 2015; Shackleton *et al.* 2003).



Increasingly cold and dry conditions culminated around 20,000 years ago during MIS 2, the Last Glacial Maximum, at which time ice sheets advanced far south into Europe and sea levels dropped 120 meters below current levels.

The Pleistocene is followed by our current geological epoch known as the Holocene, beginning 11,700 years ago (Walker *et al.* 2012). In Oman, the period between approximately 10,000 and 8,000 years ago is also referred to as the Holocene Climatic Optimum, given the generally warm and wet conditions that prevailed (Parker *et al.* 2004). This wet period was followed by a general drying trend that was punctuated by recurring century-scale megadroughts between 8,000 and 6,000 years ago, during the Middle Holocene (Preston *et al.* 2015)

The Palaeoclimatic Record and Research Paradigms

The evidence from speleothem, sedimentary and marine environmental proxy signals found throughout Oman show a number of climatic fluctuations over the course of the Quaternary period, corresponding with recurring glacial-interglacial cycles. Wet periods, triggered by the northward migration of the Inter Tropical Convergent Zone (ITCZ), activated the interior draining *wadi* systems and filled the inland playa lake basins. Studies of speleothem and lacustrine deposits suggest the onset of pluvial conditions was rapid, followed by a gradual decline in rainfall over several millennia as the ITCZ slowly returned southward.

Hence, the southern highlands encompassing Dhofar, Hadramawt and southwestern Yemen, remained under the delayed influence of a heightened rainfall regime for a longer time than inland regions (Fleitmann *et al.* 2007; Lézine *et al.* 2017).

Using these palaeoenvironmental data, researchers are able to build a framework of climate change with which to model prehistoric occupations. Massive alluvial deposits in northern Oman indicate that the climate of the early Quaternary, from two million to half a million years ago, was generally warmer and wetter than today (Blechsmidt *et al.* 2009). Oman became increasingly more arid after that, with evidence for heightened rainfall around the following times: 1) 410,000 BP, 2) 330,000-300,000 BP, 3) 220,000-200,000 BP, 4) 130,000-115,000 BP, 5) 105,000-100,000 BP, 6) 82,000-78,000 BP, 7) 60,000-40,000 BP, and 8) 10,000-8,000 BP. While the MIS 5 pluvial periods are thoroughly represented in the terrestrial and marine archives throughout all of Arabia, the evidence between 60,000 and 40,000 BP (early MIS 3) suggests only brief and ephemeral wet periods that were insufficient to trigger speleothem growth, or to fill the interior lake basins for any sustained length of time (Matter *et al.* 2015; Preusser 2009).

During pluvial periods, sea levels around the Arabian Peninsula were roughly equivalent to today, in some cases exceeding current levels by up to three meters (Macumber 2011). For the remainder of human prehistory, sea levels were reduced between 40 and 120 m (Lambeck 1996). There was an inverse correlation between the amount of annual precipitation and shoreline configuration, which is fundamental to understanding human prehistory in the Arabian Peninsula. This dynamic created a pushing and pulling mechanism from the interior grasslands to the emergent continental shelf, as these zones repeatedly cycled between habitable and uninhabitable over the course of the Pleistocene.



Figure 1.2. The Al-Hajar Mountains near Wadi Al-Ain (photograph by the authors).

Figure 1.3. Panorama of farming terraces on Jebel Akhdar (photograph by the authors).



Two different research paradigms have developed among scholars seeking to model early human demographics in the Arabian Peninsula. The first, called “*tabula rasa*”, envisions that populations could only settle in the Peninsula during pluvials and were subsequently displaced when cyclical climatic downturns caused widespread desertification (Drechsler 2007; Rose 2006; Uerpmann *et al.* 2009).

A second paradigm argues for the presence of demographic refugia, which were stable habitats around which human groups coalesced when rainfall became scarce (Bailey *et al.*, 2015; Rose, 2007, 2010). Genetic studies of modern Arabian populations point to the latter possibility, with a major ice age refugium located in South Arabia (Al-Abri *et al.* 2012; Černý *et al.* 2011; Gandini *et al.* 2016; Platt *et al.* 2017; Yang and Fu 2018).

Geographic Scope of the Dhofar Archaeological Project

Virtually the entire Pleistocene archaeological record of Oman is comprised of chipped stone waste and stone tools (lithics). The countless lithic scatters found across South Arabia are vestiges of the many successive prehistoric groups that inhabited the region. Although most artifacts found on these deflated surfaces cannot be directly dated, arid landscapes such as the Nejd Plateau provide nearly total archaeological visibility, enabling researchers to track early human tool-making activities and tool usage across the whole terrain. In this section, we present the different landscapes of southern Oman with specific attention to the Nejd Plateau. We discuss the geology of these landscapes and when various ecological niches in southern Oman would have been available to sustain human habitation during the Pleistocene.



The Sultanate of Oman

Nestled in the southeastern corner of the Arabian Peninsula, the Sultanate of Oman (Figure 1.1) is delimited by the Rub Al-Khali desert to the west, the Arabian Sea and Sea of Oman to the south and east, the Musandam Peninsula to the northwest and a land border separating Dhofar from Mahra in the southwest of Oman. The country is naturally divided into three geological zones: the Al-Hajar Mountains in northern Oman, the central plateau and the Huqf depression in the interior and the Dhofar Mountains in the southwest (Platel *et al.* 1992). The Al-Hajar Mountains form a continuous mountain range from the northern tip of the Musandam Peninsula, at the Strait of Hormuz, to its easternmost point terminating near Al-Ashkharah in the northern Ash Sharqiyah region (Figure 1.2). The Al-Hajar Mountains extends for over 700 km and rises up to 3000 m above sea level, reaching its highest points around Saih Hatat and Jebel Akhdar (Figure 1.3). A narrow coastal plain made up of alluvial and aeolian deposits intermingled with khabra deposits bounds the Al-Hajar to the northeast, while massive alluvial fans are found to the south and west.

Numerous wadis dissect the plateau, which once flowed with ancient rivers draining into the Umm as Samim and Huqf depressions (Glennie 2005). During MIS 5 and the Early Holocene Optimum, basins within the Huqf, Ash Sharqiyah and southern Rub Al-Khali were filled with perennial lakes (Matter *et al.* 2015; Radies *et al.* 2005; Rosenberg *et al.* 2012). Within the Huqf depression, there are extensive sabkha deposits created by high groundwater that form an evaporitic crust. In this region, sabkhas, palaeolake marls and stabilized dune fields are all that remain of a once productive landscape (Jagher and Pümpin 2010).



Figure 1.4. Archaeological survey near Adam in central Oman (photograph by the authors).

The Governorate of Dhofar

In the south of Oman is the Governorate of Dhofar, which is partitioned into six distinct ecological zones: 1) coastal plain, 2) seaward slopes and southern draining *wadis*, 3) summit grasslands, 4) northern mountain slopes and rain shadow, 5) plateau and canyon lands, and 6) southern Rub Al-Khali basin (Miller and Morris 1988; Raffaelli and Tardelli 2006).

Flat open desert dominates the northern part of the region, which is comprised of gravel plains, sabkhas and increasingly higher dunes as one travels deeper into the Rub Al-Khali sand sea. Vegetation across the open desert consists of generally sparse shrub communities including *Calligonum crinitum*, *Cornulaca arabica* and *Haloxylon persicum* (Mandaville 1990). The dry Nejd Plateau is rocky and hilly, increasing in elevation to the south where it abuts the Dhofar Mountains. The mountains, escarpment and interior plateau are comprised of shallow marine sediments that overlay the crystalline basement of the Arabian shelf. The horizontally bedded limestone that composes the escarpment and plateau belong to the Hadramawt geological group, which extends all the way from central Yemen. Over the course of successive Quaternary pluvial phases, the northward draining *wadis* across the Nejd have carved long, meandering river valleys through the Tertiary limestone plateau, debouching toward the Rub Al-Khali basin in the north. Stands of shrubs, acacia and ghaf trees are found along *wadi* beds, where surface runoff collects during storms. Since the introduction of center pivot irrigation in the last decade, numerous farms have sprung up in the fertile zone at the interface of the Nejd.



Figure 1.5. Salalah coastal plain with the Dhofar Mountains on the right (photograph by the authors).

The summit grasslands and seaward slopes form an orographic barrier between the monsoon-affected areas to the south and the dry plateau to the north. The grasses in this region belong to an endemic plant community of *Themeda quadrivalvis*, which is a palaeorelict outlier of the East African savannah (Patzelt 2011). The seaward slopes house woodlands and shrublands that form part of the southern Arabian cloud forest; vegetation fed by the dense moisture brought by the annual monsoon (Hildebrandt and Eltahir 2006). Arboreal species include the endemic *Anogeissus dhofarica* and *Commiphora* spp.

The coastal plain is a 50-kilometer long crescent shaped landmass stretching from Ras Raysut to Mirbat, ranging from ten to fifteen kilometers wide (Figure 1.5). It is composed of Quaternary conglomerates and alluvial fans dipping toward the coast, which are cut by short *wadis* draining into the sea. Vegetation on the coastal plain tends to be primarily composed of neophytes such as date palms, coconut palms and bananas grown on irrigated fields near the major *wadi* outlets (Platel *et al.* 1992).

On the plain stretching between Taqa and Mirbat, there a series of major faults within the Upper and Lower Hadhramawt limestone formation, which are responsible for the irregular relief of this region. Among the tertiary limestone deposits encountered in this area, the Rus formation is of considerable importance. An outcrop of this facies is found east of Taqa, within a recrystallized collapsed breccia containing chert nodules. Tectonic uplift, however, has caused the chert nodules to shatter, rendering them undesirable for knapping. East of Mirbat, the exposed crystalline basement is composed of metamorphic and plutonic rocks (Figure 1.6). Intrusive dolerite and rhyolite dykes occasionally slice across this landscape.

Figure 1.6. Landscape east of Mirbat showing rhyolite dykes (photograph by the authors).



The 1200 m high Dhofar Mountain escarpment traps moisture brought by the Indian Ocean monsoon, enveloping southern Oman in fog and rain annually between June and September. During the monsoon season, called the khareef, the southward draining *wadis* are filled with running fresh water (Figure 1.7). The major southern drainage systems include Wadis Jarzis, Arbat, Arzat, Haskeem, Darbat and Hinna. Recent to sub recent travertine deposits are found within the *wadi* valleys (Platel *et al.* 1992).

During the khareef, interdunal and coastal estuaries form along the plain. These are protected by sand barriers and typically do not connect to the ocean. Fresh water flowing from springs and major coastal *wadis* create these lagoon estuarine ecosystems, called *khawrs* (Hoorn and Cremaschi 2004). Moisture and vegetation have produced layers of soil rich in clay, covering the slopes and uplands. In addition to *Anogeissus dhofarica* woodlands found along the seaward slopes, there is a single stand of baobab trees (Figure 1.8), which may have been planted by the nearby occupants of the late Iron Age port city of Sumhuram (Aronson *et al.* 2017).

The Nejd Plateau

Given its wealth of prehistoric archaeology, our survey focused on the bare desert scabland and incised canyons that comprise the Nejd Plateau. This distinct geomorphic zone begins with small *wadis* dissecting the barren tableland at its southern extent (Figure 1.9).



In the central Nejd, the *wadis* conjoin to form wider and deeper canyons. The landscape becomes more homogeneous as the plateau dips northward, giving way to a gently undulating plain across the northern extent. Here the major catchment systems converge at the interface of the Rub Al-Khali, flowing northeastward into the basin.

The DAP survey partitioned the Nejd into eastern and western halves, with the gravel plain transecting Thumrayt serving as the boundary between the two. Each side was then divided into southern, central and northern sectors. In the south, low table mountains (mesas) and inselbergs between 5 and 20 m in elevation rise above a terrain of gravel plains and *wadi* channels (Figure 1.10).

Two main geological groups are found in the southern Nejd: 1) the Lower Hadramawt group consisting of the Umm er Radhuma and Rus formations, and 2) the Upper Hadramawt group made of the Dammam and Aydim formations. The Umm er Radhuma formation is a thick, shallow marine unit that comprises the main tertiary carbonate sequence. This grey to whitish limestone is full of large, high quality chert nodules – a prominent source of raw material for the production of stone tools throughout human prehistory.

The Rus formation is also significant for its frequent and high quality chert outcrops (Figure 1.11). Throughout the southern Nejd, the Rus formation is divided into two members; the lower chalky *Aybut* member and the upper marly-carbonated Gahit member (Platel *et al.* 1992). The *Aybut* member is a 3-5 m thick brecciated dolomitic limestone with thin yellow-orange chert nodules at the bottom. The quality and size of these nodules are highly variable. *Aybut* chert plaquettes are often highly fractured and range in size and quality. The Gahit member consists of thinly bedded, bioclastic layers of banded grey chert nodules and slabs.



Figure 1.7. Wadi Darbat during the monsoon season (photograph by the authors).



Figure 1.9. View from the Dhofar orographic barrier facing north towards the Nejd Plateau (photograph by the authors).



Figure 1.8. Vegetation on the flanks of the Dhofar Mountains (photograph by the authors).



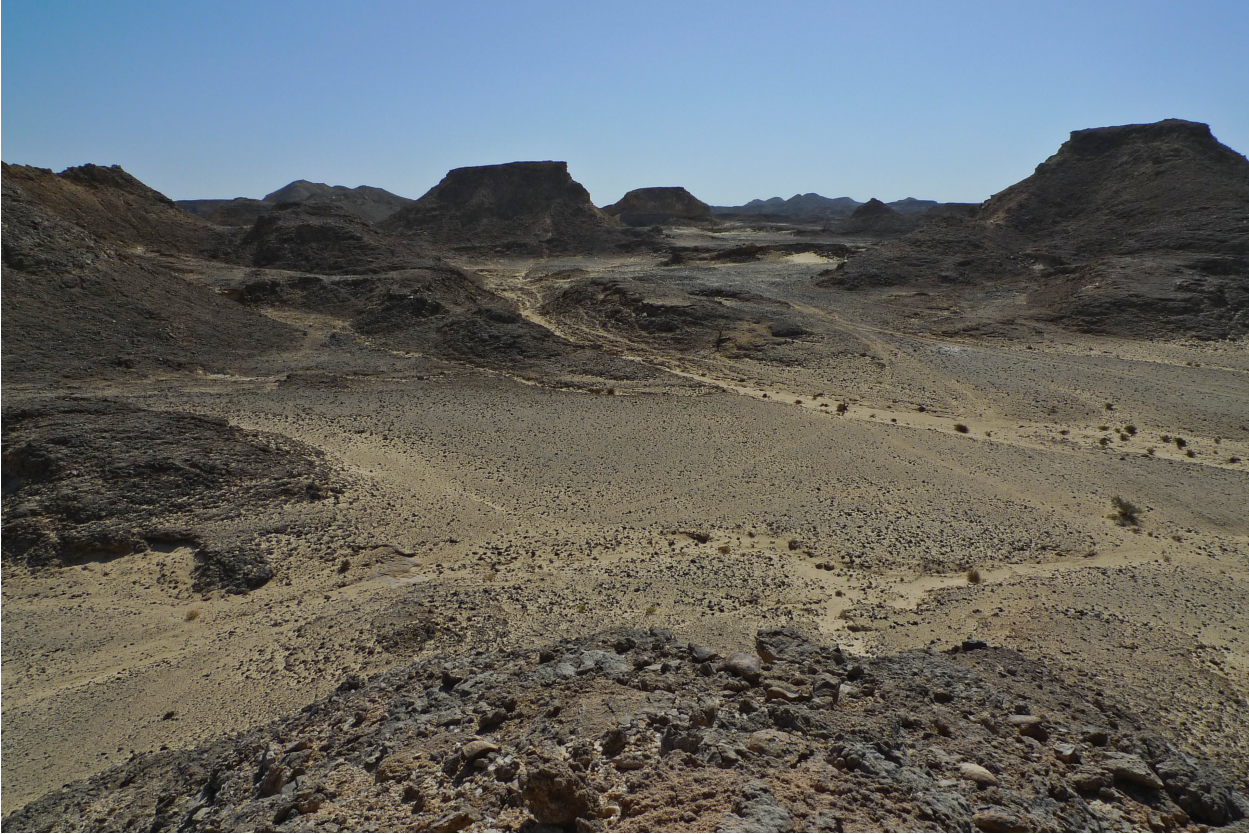


Figure 1.10. Scablands on the southern Nejd Plateau in the vicinity of Wadi Haluf (photograph by the authors).

In the region around Thumrayt, the central Nejd forms a gravel plain with patches of aeolian sediments and sparse inselbergs that are remnants of the upper Hadramawt group. These low, isolated hills often have chert slabs and nodules eroding from the scarps. The Nejd's northward draining *wadis* carry reworked aeolian and alluvial sediments downstream as they downcut during sporadic activation (Figure 1.12).

The northern Nejd is a desolate gravel plain covered by a thin veneer of aeolian sands (Figure 1.13). Prominent landscape features are ancient alluvial fans, rare travertine deposits and calcareous palaeosoils interstratified within Miocene limestone beds. Sometime in the Late Pleistocene, minor tectonic folding occurred along an east-west band in the northern Nejd, diverting stream flow and creating fracture springs (Zarins 2001). Beyond the Nejd, the Rub Al-Khali stretches to the central Arabian Peninsula, with sand dunes reaching over 200 m of height (figure 1.14). Pleistocene river systems once flowed across this interior depression, draining northeastward toward the Gulf (McClure 1976; Zarins 2001).

Summary

The fluctuating climate caused by glacial-interglacial cycles has profoundly affected the landscapes of Arabia and, consequently, early human habitation. Interglacial periods pulled the ITCZ northward, depositing rains across the interior and activating *wadis* and lake basins. Conversely, glacial phases pushed the ITCZ southward, depriving the interior of moisture. Examples of pluvial events are well documented from terrestrial and marine archives during the Last Interglacial (MIS 5.5) and to a lesser degree during MIS 5.3 and 5.1.



Figure 1.11. Raw material outcrops found across Dhofar (above); dense carpet of chert artifacts above Wadi Ghadun close to Mutahafah (below); chert nodules outcropping from the limestone bedrock of the Nejd (photographs by the authors).



Figure 1.12. Panorama over Wadi Aybut on the west-central Nejd (photograph by the authors).



Figure 1.13. The northern Nejd Plateau near Shisr Farms (photograph by J.M. Geiling).



Figure 1.14. Sand dunes north of Al-Hashman in the southern Rub Al-Khali (photograph by the authors).

The ITCZ returned northward again during the Holocene Climatic Optimum between approximately 10,000 and 8,000 years ago. These pluvial periods replenished subterranean springs, activated perennial rivers, filled lake basins and facilitated the expansion of tall-grass savannahs. With the grasslands came large herbivores including extinct giant bison, extinct straight-tusked elephants, aurochs, oryx, gazelle and wild camels (Hadjouis 2007; Rachad 2007; Stewart *et al.* 2017). These mammals, in turn, attracted apex predators such as leopards, cheetahs and humans.

While researchers believe that the onset of pluvial conditions in South Arabia was relatively abrupt, the southward migration of the ITCZ and subsequent environmental desiccation was gradual (Fleitmann *et al.* 2007; Lézine 2009; Lézine *et al.* 2017). As the ITCZ drifted southward, desertification advanced. Groundwater levels sunk, while aeolian transportation and sporadic runoff across dry terrain eroded the topsoil. The widespread savannah grasslands constricted into the Dhofar highlands (Patzelt 2011) and the large mammals that once roamed the plains dwindled and disappeared by the Middle Holocene.